Origin of Bonding Interactions in $Cu_2^+(H_2)_n$ Clusters: An Experimental and Theoretical Investigation†

Manuel J. Manard, John E. Bushnell, Summer L. Bernstein, and Michael T. Bowers*

Department of Chemistry, University of California, Santa Barbara, Santa Barbara, California 93106-9510

Received: May 2, 2002; In Final Form: July 11, 2002

Equilibrium methods were used to measure binding energies and entropies for the attachment of up to six H_2 ligands to ground-state Cu_2^+ ($^2\Sigma_g$, $3d^{20}$ σ^1). Bond dissociation energies (BDEs) of the first five H_2 ligands added to ground-state Cu_2^+ are 12.4, 10.1, 4.9, 3.8, and 2.1 kcal/mol respectively, with the BDE of the sixth ligand approximated to be 1.7 kcal/mol. Entropy measurements indicated all six of the H_2 ligands were in the first solvation shell. Theoretical calculations at the DFT-B3LYP level were done on Cu_2^+ for the first four H_2 ligands. Vibrational frequencies and geometries were determined, and the origin of the bonding and its variation with Cu_2^+ coordination was examined. Comparisons are made to the $Cu^+(H_2)_n$ and $Zn^+(H_2)_n$ systems.

Introduction

In the past 15 years, experiments conducted on gas phase transition metal ion clusters have broadened our understanding of the nature of their bonding from a simple electrostatic view to an awareness of the complex factors that are actually involved. Many of these experiments have been conducted by ligating oxidized transition metal core ions with uninserted H_2 molecules. This was first shown possible by the experiments of Kubas et al.[1] In the time that has followed, systematic experiments have examined the properties of numerous gas-phase metal ion M^+-X_n clusters. Relatively simple systems with $X = H_2$,[2−11] CO,[12−17] and methane[3,18] have been examined, along with a variety of other ligands.[19,20] The influence of the nature of the metal ion on both bonding energies and structures on these clusters clearly show the presence of covalent forces in the bonding. The large difference in M^+-X_n bond energies between the truly inert alkali ions and the transition metals reinforces this observation.[21] Additionally, the relatively small size of these clusters makes them well suited for modeling with high-level ab initio calculations. These calculations have proven necessary in order to gain a complete understanding of both the structures and the underlying bonding processes present in these systems.[19] The covalent forces present in bonding interactions with H_2 have been elucidated both by our efforts[2−11] and theoretical investigations of others.[19,22−29] The dominant electronic processes have been determined to be the following. First is the electron donation from the H_2 σ orbital to the metal, which stabilizes the ion charge.[19,25,28] Most of this donation is to the metal 4s orbital with a minor amount to the 3d orbital of the proper symmetry. Second, in the late metal ions with filled 3d orbitals, back-donation to the H_2 σ^* orbital occurs from the metal dπ orbital.[19,25−27] There are two benefits from this back-donation: greater σ donation occurs because electron density is returned to the H_2 ligand and 3d−3d exchange stabilization on the metal increases. Third, hybridization of the 3d/4s orbitals of the transition metal ion occurs in order to reduce on-axis Pauli repulsion.[19,22−28] Last, noncovalent electrostatic interactions, such as charge induced dipoles, play a role in the bonding.[19,21−24] However, interactions of this last type have been found to minimally contribute to the overall bond strength. The relative importance of these factors depends strongly on the valence configuration of the metal ion. The 4s orbital is especially critical, and its occupation is always destabilizing.[8,19,20]

To date, all of the first row transition metal $M^+(H_2)_n$ systems have been studied via temperature-dependent equilibrium measurements as well as ab initio calculations.[2−11,22−29] However, the binding of H_2 to transition metal dimer cations, $M_2^+(H_2)_n$, has not been examined. For this reason, $Cu_2^+(H_2)_n$ clusters were investigated to see how they compare with similar metal monomer clusters. It is of particular interest to see what effect the 4s valence electron in Cu_2^+ will have on the binding of H_2. Because this electron is shared between both copper atoms, the system is somewhat intermediate between the analogous monomer cation Cu^+, a $3d^{10}$ ion,[11] and Zn^+, a $3d^{10}$ $4s^1$ ion.[8] The presence of the 4s electron was found to be severely destabilizing for the bonding of Zn^+ with H_2, resulting in binding energies that are among the weakest in the first row transition metal series. These weak bonding interactions are in contrast to the $Cu^+(H_2)_n$ clusters, which have substantially larger binding energies. Furthermore, because hybridization was seen to be important in the monomer systems, it will be interesting to examine the role of hybridization in this $Cu-Cu^+$ system. Toward these ends, we present here a combined experimental and theoretical study of $Cu_2^+(H_2)_n$.

Experimental Section

A description of the instrument and experimental details has been given previously.[5,7,30] Hence, only a brief description will be given here. The Cu_2^+ ions are generated from a copper anode in a glow discharge ion source using an Ar bath gas. The preferred isotope (either $^{126}Cu_2^+$, $^{128}Cu_2^+$, or $^{130}Cu_2^+$) is then mass selected by a quadrupole mass filter and injected into a 4 cm long drift/reaction cell. The cell is typically filled with 2−4 Torr of H_2 gas. Equilibria are then quickly established as the various $Cu_2^+(H_2)_n$ clusters are drawn through the cell under the influence of a small electric field. The electric field is small enough so that the thermal energy of the ions is not significantly perturbed. The clusters exiting the cell are then mass selected by a second quadrupole and detected. Peak intensities are

† Part of the special issue "Jack Beauchamp Festschrift".

* To whom correspondence should be addressed.

10.1021/jp021105m CCC: $22.00
Published on Web 08/14/2002

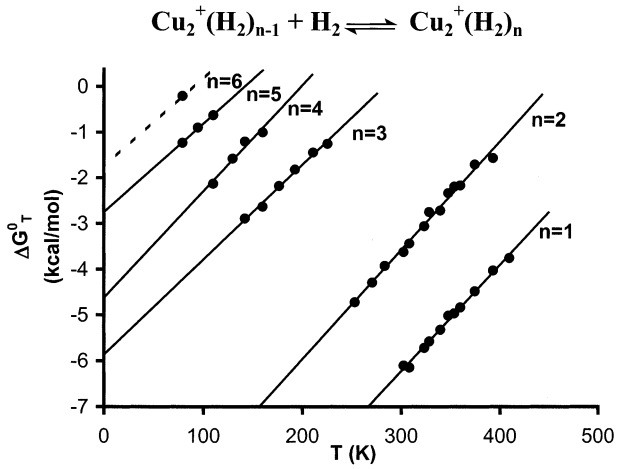

Figure 1. Plot of experimental ΔG°_T versus temperature for the association reaction of $Cu_2^+(H_2)_{n-1} + H_2 \rightleftarrows Cu_2^+(H_2)_n$. Lines are statistical mechanical fits to the data, which yield values of $-\Delta H^\circ_T$ at $T = 0$ K.

recorded and integrated, and these values, along with the pressure of H_2 (P_{H2}) in Torr, are used to determine an equilibrium constant (K°_p) for the reaction from eq 1:

$$K^\circ_p = \frac{[Cu_2^+(H_2)_n]}{[Cu_2^+(H_2)_{n-1}]} \frac{760}{P_{H_2}} \quad (1)$$

The equilibrium constant can then be used to calculate the standard Gibbs free energy of the reaction:

$$\Delta G^\circ_T = -RT \ln[K^\circ_p] \quad (2)$$

and the values obtained for ΔG°_T are plotted versus the temperature, to obtain ΔS°_T and ΔH°_T from eq 3:

$$\Delta G^\circ_T = \Delta H^\circ_T - T\Delta S^\circ_T \quad (3)$$

The resulting plots, shown in Figure 1, are approximately linear with slopes equal to the entropy (ΔS°_T) of the reaction and intercepts equal to the binding energy (ΔH°_T) of the molecule. ΔH°_0 is then determined by fitting the data using statistical thermodynamics. Vibrational frequencies and rotational constants are taken from density functional theory (DFT)[31] calculations (see next section) when available, ($Cu_2^+(H_2)_n$, $n = 1-4$). For the fifth cluster, frequencies and rotational constants are estimated by analogy with earlier clusters. In all cases, vibrational frequencies and rotational constants are varied over a wide range, and the effect on ΔH°_0 is included in the error limits. It should be stressed that uncertainties in these parameters have little effect on the final values of ΔH°_0. The bond dissociation energy (BDE) is equal to $-\Delta H^\circ_0$.

Theory

The product ions discussed here were all examined theoretically to determine the molecular parameters needed to analyze the experimental data, to identify factors important in the bonding, and to obtain structures of the clusters. Calculations were carried out at the DFT level using the B3LYP hybrid functional.[32,33] All calculations were performed using the Gaussian 98 package.[34] The basis set used in these calculations is composed as follows. The hydrogen basis set is the scaled (4s)/[2s] set of Dunning,[35] augmented with a polarization p function with an exponent of (1.2) and diffuse s (0.071) and p (0 0.4 and 0.13) functions. The optimization of these exponents is described elsewhere.[26] The copper basis set is an [8s4p3d] contraction of the (14s9p5d) primitive set proposed by Wachters[36] supplemented with two diffuse p functions (we used the Wachter's exponents[36] multiplied by 1.5), one diffuse d function,[37] and a polarization f function. This leads to a (14s11p6d3f)/[8sp4d1f] contraction.[38]

TABLE 1: Data Summary for $Cu_2^+(H_2)_{n-1} + H_2 \rightleftarrows Cu_2^+(H_2)_n$

	experiment				theory	
n	$-\Delta H^\circ_T$ [a]	$-\Delta S^\circ_T$ [b]	$-\Delta H^\circ_0$ [c]	T [d]	D_e [a]	D_0 [a]
1	13.3 ± 0.2	23.5 ± 0.7	12.4 ± 0.1	360 ± 50	12.09	9.86
2	10.7 ± 0.2	23.9 ± 0.7	10.1 ± 0.2	320 ± 70	9.90	7.84
3	5.9 ± 0.2	20.8 ± 0.9	4.9 ± 0.2	185 ± 40	6.00	3.23
4	4.6 ± 0.5	23.3 ± 3.0	3.8 ± 0.2	135 ± 25	4.23	1.88
5	2.8 ± 0.1	19.5 ± 1.0	2.1 ± 0.1	95 ± 15		
6	1.7[e]			80		

[a] In units of kcal/mol. [b] In units of cal/mol K. [c] Fitting with theoretical vibrational frequencies, rotational constants, and geometries in units of kcal/mol. [d] In Kelvin, ± refers to temperature range not uncertainty. [e] Estimate, fit by correspondence with fifth cluster, not enough data for ΔS°_T and ΔH°_T measurement.

Although the ground state of Cu_2^+ is thought to be the $3d^{20}4\sigma^1$, $^2\Sigma_g$ state[39] derived from the ground states of Cu^0 and Cu^+, $3d^{19}4\sigma^2$ excited states corresponding to the $3d^94s^1$, ^2D excited state of Cu^0 and ground-state Cu^+ were also examined and found to be greater than 25 kcal/mol higher in energy in all cases. All other excited states derive from atomic states that are at least 62 kcal/mol above the ground states and, thus, were deemed too high in energy to warrant consideration. The $3d^{19}4\sigma^2$ excited states are expected to bind more weakly to H_2 than the $3d^{20}4\sigma^1$ ground state because of the doubly occupied, repulsive σ orbital. Geometry optimizations of $Cu_2^+(H_2)_n$ clusters were performed on a wide variety of conceivable geometries in order to ascertain the true global minima. All confirmed minima contained H_2 ligands bound in a perpendicular fashion (rather than end-on) because of the orientation of the quadrupole moment of H_2.[25] Analytical frequencies were calculated for all minima, and reported frequencies are unscaled. BSSE was estimated using the counterpoise method for the formation of $Cu_2^+(H_2)_1$ and found to be less than 0.2 kcal/mol. Therefore, no further counterpoise corrections were performed, and all binding energies reported here are uncorrected for BSSE.

Results and Discussion

A summary of the experimental enthalpies and entropies as well as theoretical binding energies for the reaction $Cu_2^+(H_2)_{n-1} + H_2 \rightleftarrows Cu_2^+(H_2)_n$ are given in Table 1. Calculated vibrational frequencies are listed in Table 2. All of the cluster ions discussed here consist of an intact Cu_2^+ core ion surrounded by largely unperturbed H_2 ligands. No evidence of insertion to form a dihydride was found.

$Cu_2^+(H_2)$. The first H_2 ligand adds side on to the Cu_2^+ ion in C_{2v} symmetry (Figure 2). The experimental ΔH°_T and ΔS°_T values for $Cu_2^+(H_2)$ are -13.3 kcal/mol and -23.5 cal/mol K, respectively. Figure 1 shows both the experimental free energy (points) and those calculated from statistical thermodynamics using theoretically determined vibrational frequencies (Table 2) and rotational constants (lines). The BDE of $Cu_2^+(H_2)$ is 12.4 kcal/mol. The calculated (DFT) binding energy (D_0) for this system is 9.86 kcal/mol or approximately a 20% underestimation of the binding energy. However, this error is consistent with the variance associated with the theoretical binding energies of previous transition metal systems, including Cu^+ and Zn^+. The

TABLE 2: Theoretical Vibrational Frequencies for $Cu_2^+(H_2)_n$ Clusters[a,b]

	Cu−Cu sym. stretch	H−H stretch	$Cu_2^+-H_2$ sym. stretch	$Cu_2^+-H_2$ asym stretch	$H_2-Cu_2^+-H_2$ bends and rotations	internal rotations
$Cu_2^+(H_2)_1$	170	3899	772	1070	97, 151	
$Cu_2^+(H_2)_2$	157	3938, 3935	712, 681	1001 (2) 139, 150	87, 105,	119
$Cu_2^+(H_2)_3$	151	3873[c], 3881 3950	677, 653, 668	973, 1010, 1031	95, 114, 143, 183, 235,	115, 315, 316
$Cu_2^+(H_2)_4$	148	3884, 3894, 3883 3894	633, 636(2), 621	979(2), 999, 1006	91, 101(2), 185(2), 225, 246,	319(2), 324, 326
Cu_2^+	179					
H_2		4422				

[a] Harmonic vibrational frequencies for the different $Cu_2+(H_2)_n$ clusters as obtained by analytical differentiation of the SCF energy at SCF geometry. [b] All number in cm^{-1}. [c] Angled H_2 pair.

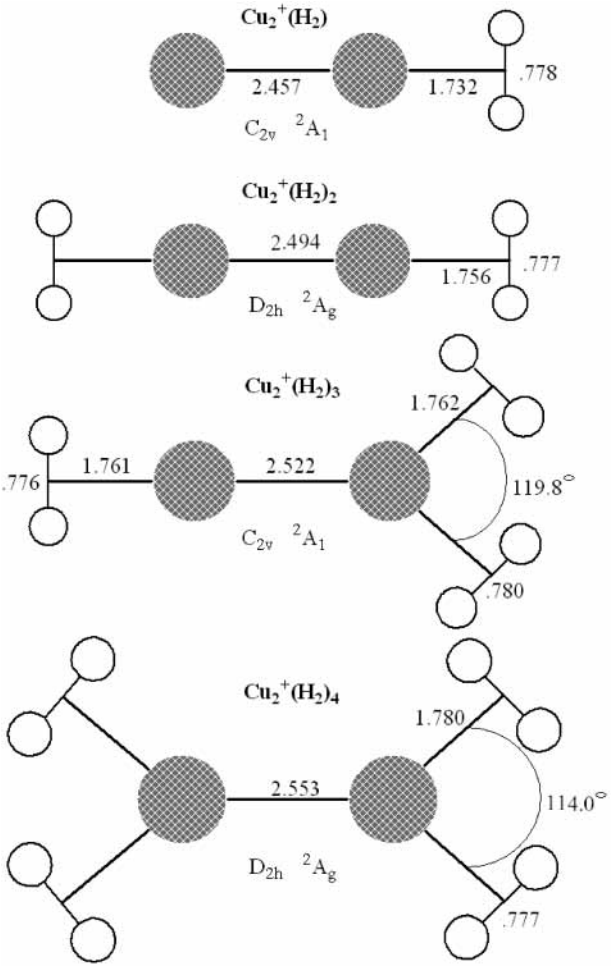

Figure 2. Theoretical geometries of the $Cu_2^+(H_2)_{1-4}$ ions calculated at the DFT B3LYP level. All distances are in angstroms. The *yz* plane is represented by the plane of the page with the *z* axis, the principal symmetry axis.

calculated $Cu_2^+-H_2$ bond distance is 1.73 Å with an associated H−H bond distance of 0.78 Å.

The $Cu_2^+(H_2)$ cluster showed bonding trends that were intermediate between those of $Cu^+(H_2)$[11] and $Zn^+(H_2)$.[8] However, because the nature of the bonding in $Cu^+(H_2)$ and $Zn^+(H_2)$ is vastly different, with $Cu^+(H_2)$ boasting a largely covalent bond 4 times stronger than that of the more electrostatic bond of $Zn^+(H_2)$, it is of interest to determine which aspects of $Cu_2^+(H_2)$ bonding interactions mimic those of $Cu^+(H_2)$ and which resemble those of $Zn^+(H_2)$. Accordingly, we first note that the $Cu_2^+-H_2$ bond length is nearly identical to that of $Cu^+(H_2)$ and that the BDE of $Cu_2^+(H_2)$ is only about 3 kcal/mol smaller than that of $Cu^+(H_2)$. In contrast, the BDE of $Cu_2^+(H_2)$ is larger than that of $Zn^+(H_2)$ by approximately 8.5 kcal/mol, suggesting the bonding in $Cu_2^+(H_2)$ is predominately covalent. It also indicates that, although the σ(4s) electron of the Cu_2^+ ion does slightly weaken the bonding in the system compared to that of $Cu^+(H_2)$, it does not destabilize the bonding as much as the 4s electron on Zn^+ does in the $Zn^+(H_2)$ cluster. The corresponding association entropies of $Cu_2^+(H_2)$ and $Cu^+(H_2)$ (−23.5 and −19.7 cal/mol K, respectively) are also similar and larger than that of $Zn^+(H_2)$ (−14.4 cal/mol K), further illustrating that $Cu_2^+(H_2)$ is a more tightly bound ion.

The remaining bonding characteristics of $Cu_2^+(H_2)$ could be mainly attributed to the σ(4s) electron. The σ(4s) electron of Cu_2^+ differs from the 4s electron of Zn^+ in the role it plays in bonding in several ways. First, although both the σ(4s) and 4s electron increase on-axis Pauli repulsion in the two respective systems when compared to the unoccupied 4s orbital of Cu^+, the increased repulsion in the Cu_2^+ system is significantly smaller than that of Zn^+. This is due to the nature of the Cu−Cu σ(4s) bond. Because the σ(4s) electron is shared between two Cu atoms, it is possible for the electron density to be delocalized and shifted farther away from a bonding H_2 molecule than would be possible for an atomic ion with a 4s valence electron. Calculations indicate a shorter $M_n^+-H_2$ bond length in $Cu_2^+(H_2)$ than in $Zn^+(H_2)$ in support of this suggestion.

Second, σ donation from H_2 to the σ(4s) orbital of Cu_2^+, though smaller than H_2 σ donation to the 4s orbital of Cu^+, is significantly larger than that of H_2 σ donation to the 4s orbital of $Zn^+(H_2)$. This is attributed to two effects: (1) the σ (4s) Cu_2^+ and σ H_2 orbital overlap is greater than the 4s Zn^+ and σ H_2 orbital overlap because of the reduced $M_n^+-H_2$ bond length in $Cu_2^+-H_2$ and (2) the delocalized charge density of the σ(4s) electron of Cu_2^+ does not hinder H_2 σ donation as much as the 4s electron of Zn^+. Theory indicates that the charge density of the $Cu_2^+(H_2)$ σ(4s) electron is polarized away from the H_2 ligand, increasing the strength of the bond. In contrast, the electronic charge density of Zn^+ is highly localized in the 4s orbital and cannot as readily be shifted away from the H_2 ligand in order to reduce on-axis Pauli repulsion.

Third, the shorter $Cu_2^+-H_2$ bond length also reflects the increased 3dπ back-donation from Cu_2^+ to the σ^* orbital of H_2. NBO population analysis[40] indicates that electron density is considerably decreased in the $3d_{yz}$ orbital of the Cu atom in Cu_2^+ bound to the H_2 ligand. This is the orbital from which back-donation to the H_2 ligand occurs. This effect is not unlike back-donation occurring in the $Cu^+(H_2)$ system. Both systems show similar increases in the H−H bond length and decreased H−H stretching frequencies relative to free H_2, suggesting that the amount of M_n^+ 3dπ back-donation is also similar in both systems. In contrast, $Zn^+(H_2)$ shows an H−H bond length and

stretching frequency similar to those of free H_2, indicating reduced back-donation in comparison to both copper systems.

Another aspect of $Cu_2^+(H_2)$ bonding is the use of $3d_{z^2}/4s$ hybridization to further reduce on-axis repulsion. Calculations indicate that electron density is promoted from the filled $3d_{z^2}$ orbitals on both Cu atoms to the σ(4s) orbital in both the bare ion and $Cu_2^+(H_2)$. This hybridization serves to further strengthen the bonding in the $Cu_2^+(H_2)$ cluster. Calculations also show the presence of a small amount of electron density in orbitals of $4p_z$ character in the $Cu_2^+(H_2)$ system. The $4p_z$ orbital was found to have played an important role in the bonding of $Zn^+(H_2)$.[8] However, unlike $Zn^+(H_2)$, only a minute amount of electron density is found in orbitals of $4p_z$ character in $Cu_2^+(H_2)$. This is due to the fact that the 4p orbitals lie very high in energy for first row transition metals[19] and that there are more favorable options for migration of destabilizing electron density in $Cu_2^+(H_2)$ than in $Zn^+(H_2)$, specifically polarization of electron density within the Cu−Cu σ(4s) orbital.

$Cu_2^+(H_2)_2$. The second H_2 ligand binds opposite the first in D_{2h} symmetry. The experimental ΔH_T° and ΔS_T° values for $Cu_2^+(H_2)_2$ are −10.7 kcal/mol and −23.9 cal/mol K, respectively. The BDE of $Cu_2^+(H_2)_2$ was determined by fitting theoretical and experimental ΔG_T° versus temperature curves and found to be 10.1 kcal/mol. The calculated (DFT) binding energy (D_0) for the second cluster is 7.84 kcal/mol, which is in reasonable agreement with the experimental value. The theoretical structure for $Cu_2^+(H_2)_2$ is shown in Figure 2, and the theoretical vibrational frequencies are listed in Table 2. The calculated $Cu_2^+-H_2$ bond distances are 1.75 Å with associated H−H bond distances of 0.77 Å. These values are essentially equivalent to those of the first cluster. A potential energy surface (PES) of the relative energy of the system versus the angle produced by rotating one of the H_2 ligands starting at 0° (D_{2h} symmetry) and rotating through 90° (D_{2d} symmetry) was calculated. The energy difference between the staggered and eclipsed configurations is less that 0.02 kcal/mol, indicating free internal rotation in the system. Frequency calculations on both staggered and eclipsed geometries gave all positive eigenvalues indicating true local minima.

The $Cu_2^+-H_2$ bonding interactions in $Cu_2^+(H_2)_2$ are fundamentally the same as $Cu_2^+(H_2)$, with H_2 σ donation to the σ-(4s) orbital of Cu_2^+ and $3d\pi$ back-donation from Cu_2^+ to the σ^* orbital of H_2. The BDE of $Cu_2^+(H_2)_2$ is 2.3 kcal/mol less than the BDE of the first H_2 ligand. This is in contrast to first row transition metal cations with d^n electron configurations (including Cu^+ but excluding Zn^+) where it was found that the second H_2 ligand binds stronger than the first. The phenomenon of increased BDE with addition of the second H_2 molecule in these systems arises from hybridization of the $3d\sigma$ orbital and the empty 4s orbital that occurs with addition of the first H_2 ligand to reduce on-axis Pauli repulsion. When the second H_2 binds, the cost of hybridization is shared between both of the ligands, producing a larger BDE for the second ligand. This is not the case in systems such as $Cu_2^+(H_2)_2$ where the σ(4s) orbital is singly populated. Here, much like the singly occupied 4s orbital of $Zn^+(H_2)_2$, addition of the first ligand polarizes the repulsive electron density in orbitals of 4s character away from the ligand. However, addition of the second ligand must now occur in a region of relatively high electron density. As expected, the effect of this process is a decrease in bond strength because of the energy cost of "repolarizing" the system toward its original distribution.

Although both $Cu_2^+(H_2)_2$ and $Zn^+(H_2)_2$ experience reduced bond strength with addition of the second H_2, the BDE of $Cu_2^+(H_2)_2$ is more than 7 kcal/mol stronger than the BDE of $Zn^+(H_2)_2$. The difference between these two systems arises from the fact that the majority of the Cu_2^+ σ(4s) electron density remains in the Cu−Cu σ(4s) orbital, whereas in Zn^+, substantial promotion into the $4p_x$ and $4p_y$ orbitals occurs. This can readily be seen in the NBO population analysis which indicates that there is virtually no electron density present in the $4p_x$ and $4p_y$ orbitals of Cu_2^+. This result is consistent with the calculated (DFT) geometry of the cluster, which specifies that the H_2 molecules are positioned 180° from each other on the Cu−Cu bonding axis. This linear conformation of $Cu_2^+(H_2)_2$ also indicates that the $4p_x$ and $4p_y$ orbitals play essentially no role in the bonding ($4p_x$ and $4p_y$ orbitals tend to give rise to a bent conformation much like that of $Zn^+(H_2)_2$). As previously stated, hybridization of electron charge density into the 4p orbitals of first row transition metals is always energetically costly.[19] The ability of $Cu_2^+(H_2)_2$ to avoid this process by usage of the available space of the Cu−Cu σ(4s) orbital gives rise to the stronger bonding reflected in the increased BDE when compared to $Zn^+(H_2)_2$.

$Cu_2^+(H_2)_3$. The calculated structure of the $Cu_2^+(H_2)_3$ ion is shown in Figure 2. The experimental ΔH_T° and ΔS_T° values for $Cu_2^+(H_2)_3$ are −5.9 kcal/mol and −20.8 cal/mol K, respectively. From the usual analysis of ΔG_T° versus T data (Figure 1), the BDE of $Cu_2^+(H_2)_3$ was found to be 4.9 kcal/mol. The calculated (DFT) binding energy (D_0) is 3.23 kcal/mol, in reasonable agreement with the experimental BDE. Of particular importance is the fact that the DFT calculations mirror the large reduction in bond strength observed in the experimental BDE with the addition of the third H_2 ligand. Theoretical vibrational frequencies are shown in Table 2.

The geometry of $Cu_2^+(H_2)_3$ is unique when compared to the third clusters of both the Cu^+ and Zn^+ systems. The planar C_{2v} structure of $Cu_2^+(H_2)_3$ differs from the highly symmetric D_{3h} symmetry of $Cu^+(H_2)_3$ and the nonplanar C_3 structure of $Zn^+(H_2)_3$. However, the third cluster geometries of all of these systems arise for essentially the same reason,[8,11] specifically, to minimize repulsive σ interactions of the three H_2 ligands with the electron density of the M_n^+ transition metal core ion. Once again, dissimilarities between the systems occur because of the valence shell electron configuration of the transition metal centers. In the case of $Cu^+(H_2)_3$, the geometry arises primarily from hybridization of the empty 4s orbital and the filled 3d orbitals in order to reduce repulsive σ interaction with the third H_2 ligand and the Cu^+ 3d orbitals.[11] In the case of $Zn^+(H_2)_3$, the geometry reflects the repulsive effects of the singly occupied 4s orbital and the use the 4p orbitals to reduce σ repulsion from the H_2 ligands.[8] Here, each H_2 molecule interacts with one of the 4p orbitals of Zn^+ giving rise to the nonplanar, near 90° bond angles between the H_2 ligands. The geometry of $Cu_2^+(H_2)_3$ arises from polarization of the σ(4s) electron density away from the angled H_2 ligands that are bound to the same copper atom. The $H_2-Cu^+-H_2$ angle formed by this pairing is approximately 120°. This bond angle suggests that $Cu_2^+(H_2)_3$ behaves as a typical trigonal planar molecule and uses the 120° bond angle to maximize separation between the H_2 ligands.

Thus far, bonding in the previous Cu_2^+ clusters has consisted primarily of H_2 σ donation to the σ(4s) orbital of Cu_2^+ and back-donation from the $3d\pi$ orbital of Cu_2^+ to the σ^* orbital of H_2. However, the trigonal planar conformation of $Cu_2^+(H_2)_3$ signifies a departure from the aforementioned bonding interactions and accounts for the large reduction in BDE with addition of the third H_2 ligand. Here, the two angled H_2 ligands bound to the same side of Cu_2^+ are oriented in a manner that is

best suited for σ donation to the $3d_{yz}$ orbital on the copper atom. In order for this to happen, a series of hybridizations must take place. (1) Electron density must be removed from the filled $3d_{yz}$ orbital on this Cu atom and promoted into the σ(4s) orbital of Cu_2^+. This hybridization decreases the on-axis repulsion with the angled H_2 ligands and allows for H_2 σ donation to the $3d_{yz}$ orbital. (2) Hybridization of the $3d_{z^2}$ and the $3d_{x^2-y^2}$ orbitals of the target Cu atom also occurs. This hybridization gives rise to a $3d_{y^2-z^2}$ orbital, which is now symmetry adapted for back-donation of electron density into the σ* orbitals of both H_2 ligands.

Although the bonding interactions of the doubly ligated Cu atom have changed, bonding for the H_2 ligand on the singly ligated copper center is essentially unchanged. However, polarization of the σ(4s) electron density toward this singly ligated H_2 causes reduced σ donation from the ligand. Evidence for the decrease is reflected by the increased $Cu_2^+-H_2$ bond length for this H_2 ligand. The reduced σ donation along with the hybridizations that occur in $Cu_2^+(H_2)_3$ explain the drastic reduction in bond strength. However, the BDE of the third ligand in $Cu_2^+(H_2)_3$ is still slightly stronger than that of the third H_2 ligand in $Zn^+(H_2)_3$, because the high energy 4p orbitals are not involved in the bonding.

$Cu_2^+(H_2)_4$. The calculated structure of $Cu_2^+(H_2)_4$ is shown in Figure 2. The experimental ΔH_T° and ΔS_T° values for $Cu_2^+(H_2)_4$ are -4.6 kcal/mol and -23.3 cal/mol K, respectively. The BDE of $Cu_2^+(H_2)_4$, determined in the usual fashion, is 3.8 kcal/mol. The calculated (DFT) binding energy (D_0) for this cluster is 1.88 kcal/mol. Theoretical vibrational frequencies for the fourth cluster of Cu_2^+ are given in Table 2.

The binding interactions of $Cu_2^+(H_2)_4$ can essentially be understood by combining the explanations for the bonding of $Cu_2^+(H_2)_2$ and $Cu_2^+(H_2)_3$. The addition of the fourth H_2 ligand causes the σ(4s) electron density of Cu_2^+ to be symmetrically shared between the Cu atoms in the σ(4s) orbital, giving rise to a symmetrical structure much like that of $Cu_2^+(H_2)_2$. The fourth H_2 ligand also binds in an angled fashion, much like the third H_2 ligand of $Cu_2^+(H_2)_3$. In order for this to occur, hybridizations similar to those in $Cu_2^+(H_2)_3$ must take place in $Cu_2^+(H_2)_4$. These factors combined give rise to the D_{2h} symmetry of $Cu_2^+(H_2)_4$ with a calculated $H_2-Cu_2^+-H_2$ bond angle of 114°.

The reduction in bond strength is an obvious consequence of the hybridizations that occur for $Cu_2^+(H_2)_4$ with the addition of the fourth H_2 ligand. Increased H_2 σ repulsion as well as decreased σ donation to Cu_2^+ also account for the reduced bond strength of the fourth cluster. This is consistent with the longer $Cu_2^+-H_2$ bond lengths of the calculated $Cu_2^+(H_2)_4$ structure compared to those of the previous Cu_2^+ clusters.

$Cu_2^+(H_2)_5$/$Cu_2^+(H_2)_6$. Limited data for the $Cu_2^+(H_2)_5$ cluster could only be obtained at very low temperatures (110−80 K). The experimental ΔH_T° and ΔS_T° values are -2.8 kcal/mol and -19.5 cal/mol K, respectively. The similarity of this entropy change with the previous Cu_2^+ clusters indicates that the first solvation sphere is still being filled (see ref 11). The BDE of the fifth cluster is 2.1 kcal/mol. Because of the low binding energies of $Cu_2^+(H_2)_5$, DFT calculations were not performed. The theoretical vibrational frequencies used in the fitting of the experimental $Cu_2^+(H_2)_5$ data were generated through analogy with the previous clusters. The BDE of $Cu_2^+(H_2)_5$ is 1.1 kcal/mol stronger than the BDE of $Cu^+(H_2)_5$, which had a measured BDE of 1 kcal/mol. This is the first Cu_2^+ cluster to bind stronger than the analogous Cu^+ cluster. This is due to the fact that the monomer system adds a fifth H_2 ligand in the second solvation sphere, (reflected in the increase in ΔS_T°), whereas the dimer system continues to add the fifth H_2 ligand in the first solvation sphere.

Data for $Cu_2^+(H_2)_6$ could only be taken at 80 K. These data points were matched with the slope of the Cu_2^+ fifth cluster in order to produce an estimated BDE of 1.7 kcal/mol for $Cu_2^+(H_2)_6$. Again, because of the low binding energy of the sixth cluster, DFT calculations were not performed. However, one possible configuration for $Cu_2^+(H_2)_6$ could be quasitetrahedral about each Cu center (similar to $Cu^+(H_2)_4$) with the second Cu atom taking the place of the fourth H_2 molecule.

Conclusions

1. Bond dissociation energies and association entropies were determined for $Cu_2^+(H_2)_{1-6}$. The Cu_2^+ BDEs are (in order of cluster size) 12.4, 10.1, 4.9, 3.8, 2.1, and ~1.7 kcal/mol.

2. Density functional theory calculations (B3-LYP parametrization) were done on $Cu_2^+(H_2)_{1-4}$ to obtain theoretical BDEs, geometries, rotational constants, and vibrational frequencies. Agreement between the theoretical and experimental BDEs is in all cases reasonable, with experimental trends being predicted by theory.

3. Bonding in the clusters consists mainly of donation to Cu_2^+ from the H_2 σ orbital and back-donation from the Cu_2^+ $3d\pi$ orbitals to the H_2 σ* orbital. However, in the larger clusters, H_2 σ donation to the $3d_{yz}$ orbital of Cu_2^+ with back-donation from the hybrid $3d_{y^2-z^2}$ of Cu_2^+ to the σ* orbital of H_2 occurs.

4. The bonding interactions of the $Cu_2^+(H_2)_n$ cluster ions were found to resemble aspects of the bonding interactions of both the $Cu^+(H_2)_n$ and the $Zn^+(H_2)_n$ systems. This is attributed to the valence shell electron configuration of the Cu_2^+ ion ($3d^{20}$ σ^1). The σ(4s) electron that is shared between the two copper atoms is intermediate between the electron configuration of Cu^+ ($3d^{10}$) and Zn^+ ($3d^{10}$ $4s^1$). Although the σ(4s) electron of the Cu_2^+ is found to be destabilizing when compared to the Cu^+ system, it was not as destabilizing as the 4s electron of the Zn^+ system.

Acknowledgment. The support of the National Science Foundation under Grants CHE-9729146 and CHE-0140215 is gratefully acknowledged. MTB thanks JLB for early collaborations in transition metal chemistry and acknowledges his wisdom in leaving the field before heavy metal poisoning became serious! Welcome to your seventh decade.

References and Notes

(1) Kubas, G. J.; Ryan, F. F.; Swanson, B. I.; Vergamini, P. J.; Wasserman, H. J. *J. Am. Chem. Soc.* **1984**, *106*, 451.
(2) Bushnell, J. E.; Kemper, P. R.; von Helden, G.; Bowers, M. T. *J. Phys. Chem.* **1993**, *97*, 52.
(3) Kemper, P. R.; Bushnell, J.; van Koppen, P. A. M.; Bowers, M. T. *J. Phys. Chem.* **1993**, *97*, 1810.
(4) Bushnell, J. E.; Kemper, P. R.; Bowers, M. T. *J. Phys. Chem.* **1993**, *97*, 11628.
(5) Kemper, P. R.; Bushnell, J.; Maitre, P.; Bowers, M. T. *J. Am. Chem. Soc.* **1994**, *116*, 9710.
(6) Bushnell, J. E.; Kemper, P. R.; Bowers, M. T. *J. Phys. Chem.* **1995**, *99*, 15602.
(7) Kemper, P. R.; Weis, P.; Bowers, M. T. *Int. J. Mass Spectrom. Ion Phys.* **1997**, *160*, 17.
(8) Weis, P.; Kemper, P. R.; Bowers, M. T. *J. Phys. Chem. A* **1997**, *101*, 2809.
(9) Bushnell, J. E.; Kemper, P. R.; Maitre, P.; Bowers, M. T. *J. Chem. Phys.* **1997**, *106*, 10153.
(10) Kemper, P. R.; Weis, P.; Bowers, M. T. *Chem. Phys. Lett.* **1998**, *293*, 503.
(11) Kemper, P. R.; Weis, P.; Bowers, M. T.; Maitre, P. *J. Am. Chem. Soc.* **1998**, *120*, 13494.
(12) Sievers, J. R.; Armentrout, P. B. *J. Phys. Chem.* **1995**, *99*, 8135.

(13) Khan, F. A.; Clemmer, D. E.; Schultz, R. H.; Armentrout, P. B. *J. Phys. Chem*. **1993**, *97*, 7978.
(14) Schultz, R. H.; Crellin, K. C.; Armentrout, P. B. *J. Am. Chem. Soc*. **1991**, *113*, 8590.
(15) Goebel, S.; Haynes, C. L.; Khan, F. A.; Armentrout, P. B. *J. Am. Chem. Soc*. **1995**, *117*, 6994.
(16) Khan, F. A.; Steele, D. L.; Armentrout, P. B. *J. Phys. Chem*. **1995**, *99*, 7819.
(17) Meyer, F.; Chen, Y. M.; Armentrout, P. B. *J. Am. Chem. Soc*. **1995**, *117*, 4071.
(18) Van Koppen, P. A. M.; Bushnell, J.; Kemper, P. R.; Bowers, M. T. *J. Am. Chem. Soc*. **1995**, *117*, 2098.
(19) For a general discussion, see: Bauschlicher, C. W.; Partridge, H.; Langhoff, S. R. In *Organometallic Ion Chemistry*; Freiser, B. S., Ed.; Kluwer Academic: Dordrecht, The Netherlands, 1996.
(20) Kemper, P. R.; Hsu, M. T.; Bowers, M. T. *J. Phys. Chem*. **1991**, *95*, 10600.
(21) Bushnell, J. E.; Kemper, P. R.; Bowers, M. T. *J. Phys. Chem*. **1994**, *98*, 2044.
(22) Bauschlicher, C. W.; Partridge, H.; Langhoff, S. R. *J. Chem. Phys*. **1989**, *91*, 4733.
(23) Bauschlicher, C. W.; Partridge, H.; Langhoff, S. R. *Chem. Phys. Lett*. **1990**, *165*, 272.
(24) Partridge, H.; Bauschlicher, C. W.; Langhoff, S. R. *J. Phys. Chem*. **1992**, *96*, 5350.
(25) Bauschlicher, C. W.; Partridge, H.; Langhoff, S. R. *J. Phys. Chem*. **1992**, *96*, 2475.
(26) Maitre, P.; Bauschlicher, C. W. *J. Phys. Chem*. **1993**, *97*, 11912.
(27) Perry, J. K.; Ohanessian, B.; Goddard, W. A. *J. Phys. Chem*. **1993**, *97*, 5238.
(28) Maitre, P.; Bauschlicher, C. W. *J. Phys. Chem*. **1995**, *99*, 3444.
(29) Maitre, P.; Bauschlicher, C. W. *J. Phys. Chem*. **1995**, *99*, 6836.
(30) Kemper, P. R.; Bowers, M. T. *J. Am. Soc. Mass Spectrosc*. **1990**, *1*, 197.
(31) (a) Hohenberg, P.; Kohn, W. *Phys. Rev*. **1964**, *136*, B864. (b) Kohn, W.; Sham, L. J. *Phys Rev*. **1965**, *140*, A1133.
(32) Stevens, P. J.; Devlin, F. J.; Chablowski, C. F.; Frisch, M. J. *J. Phys. Chem*. **1994**, *98*, 11623.
(33) (a) Becke, A. K. *J. Chem. Phys*. **1993**, *98*, 5648. (b) Becke, A. D. *Phys. Rev. A* **1988**, *38*, 3098. (c) Lee, C.; Yang, W.; Parr, R. G. *Phys. Rev. B*. **1988**, *37*, 785.
(34) Frisch, M. J.; Trucks, G. W.; Schlegel, H. B.; Scuseria, G. E.; Robb, M. A.; Cheeseman, J. R.; Zakrzewski, V. G.; Montgomery, J. A., Jr.; Stratmann, R. E.; Burant, J. C.; Dapprich, S.; Millam, J. M.; Daniels, A. D.; Kudin, K. N.; Strain, M. C.; Farkas, O.; Tomasi, J.; Barone, V.; Cossi, M.; Cammi, R.; Mennucci, B.; Pomelli, C.; Adamo, C.; Clifford, S.; Ochterski, J.; Petersson, G. A.; Ayala, P. Y.; Cui, Q.; Morokuma, K.; Malick, D. K.; Rabuck, A. D.; Raghavachari, K.; Foresman, J. B.; Cioslowski, J.; Ortiz, J. V.; Stefanov, B. B.; Liu, G.; Liashenko, A.; Piskorz, P.; Komaromi, I.; Gomperts, R.; Martin, R. L.; Fox, D. J.; Keith, T.; Al-Laham, M. A.; Peng, C. Y.; Nanayakkara, A.; Gonzalez, C.; Challacombe, M.; Gill, P. M. W.; Johnson, B. G.; Chen, W.; Wong, M. W.; Andres, J. L.; Head-Gordon, M.; Replogle, E. S.; Pople, J. A. *Gaussian 98*, revision A.7; Gaussian, Inc.: Pittsburgh, PA, 1998.
(35) Dunning, T. H. *J. Chem. Phys*. **1970**, *53*, 2823.
(36) Wachters, A. J. H. *J. Chem. Phys*. **1970**, *52*, 1033.
(37) Hay, P. J. *J. Chem. Phys*. **1977**, *66*, 4377.
(38) Bauschlicher, C. W. *Theor. Chim. Acta* **1995**, *92*, 183.
(39) Sappey, A. D.; Harrington, J. E.; Weisshaar, J. C. *J. Chem. Phys*. **1989**, *91*, 3854.
(40) Reed, A. E.; Curtis, L. A.; Weinhold, F. *Chem. Rev*. **1988**, *88*, 899 and references therein.